

LightVault: A Design and Robotic Fabrication Method for Complex Masonry Structures

Stefana Parascho^{1,*}, Isla Xi Han¹, Alessandro Beghini², Masaaki Miki³, Samantha Walker², Edvard P.G. Bruun^{1,4}, Sigrid Adriaenssens⁴

¹ CREATE Laboratory, Princeton University, NJ, 08544, United States

* Corresponding author e-mail: parascho@princeton.edu

² Skidmore, Owings & Merrill, One Maritime Plaza, San Francisco, CA, 94111, United States

³ The University of Tokyo, 7 Chome-3-1 Hongo, Bunkyo City, Tokyo 113-8654, Japan

⁴ Form Finding Lab, Princeton University, NJ, 08544, United States

Abstract

This paper presents a novel approach to masonry construction: utilising cooperating robots to construct complex doubly-curved vault geometries while eliminating the need for false- or formwork. An integrated design method that was developed, which takes into account both robotic and structural constraints and includes the following steps: (1) the overall design volume is defined based on the robots' position, reach, and collision constraints; (2) a form-finding approach using Airy's stress function is used to generate the target geometry; (3) the geometry is tessellated into a herringbone brick pattern; (4) the robotic construction sequence is defined based on stability and reachability constraints.

Parallel to the development of the design methodology, the paper presents the physical prototyping and implementation of the robotic assembly process. The fabrication process uses a cooperative assembly technique in which robots alternate between placement and support to first build a stable central arch. Subsequently, the construction is continued individually by the robots - building out from the central arch following an interlocking herringbone brick sequence. This methodology is implemented in a full-scale vault (3.6m x 6.5m x 2.2m) structure consisting of 338 glass bricks, built using two large-scale industrial robotic arms.

Keywords: Robotic Fabrication, Cooperative Assembly, Scaffold-Free Construction, Masonry Vault, Tessellation, Fabrication-Informed Design, Structural Form-Finding

1 Introduction

The ubiquity of digital tools and 3D visualisation software allows the modern designer nearly limitless possibilities in the type of geometries that can be envisioned. Improvements in analysis and form-finding tools mean that these complex geometries can be further refined for material and structural efficiency. On the other hand, developments in digital fabrication, such as robotic assembly, have allowed for more and more complex geometries to be successfully materialised. However, it is still difficult to combine the structural efficiency gained from form-found complex geometries with the precision of robotic fabrication techniques due to the gap in the traditionally hierarchical design and construction process. Fabrication methods are often developed without structural design in mind and vice-versa. The goal of our research is to bridge this gap between design and robotic construction. It is here that geometry and the definition of design parameters can overcome the limitations of traditional design and bring structure and fabrication closer together.

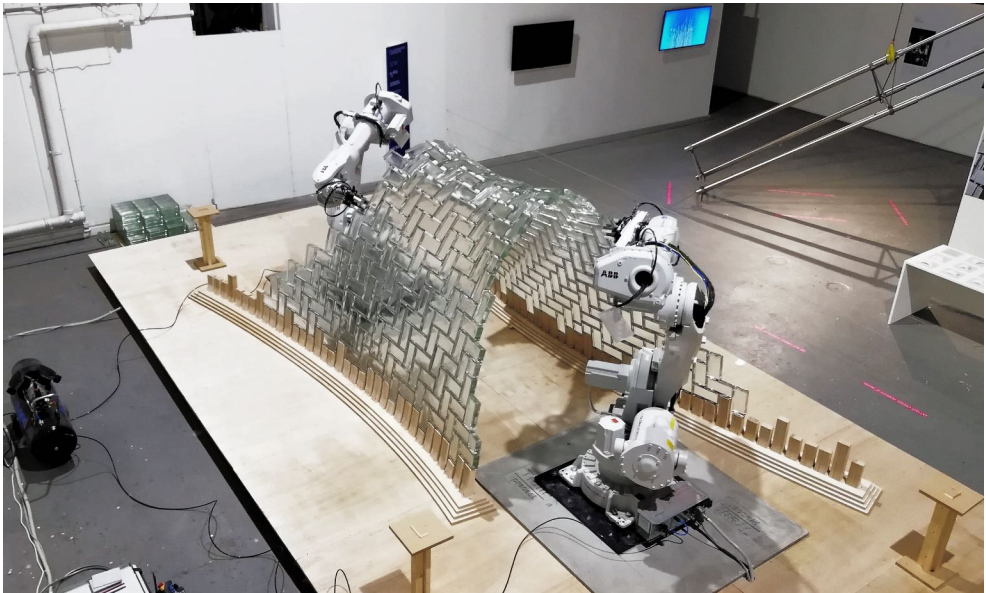


Figure 1: Robotically assembled glass brick vault.

Recent decades have seen a resurgence of interest in masonry and discrete element geometries. The work ranges from examining traditional methods of construction to novel mathematical methods for modelling and geometry optimization (Livesley 1992; Whiting 2012; Frick et al. 2015; Block and Ochsendorf 2007). But while optimised free-form masonry geometries can be calculated, as their complexity increases so does the need for temporary scaffolding, geometric templates, or skilled masons. This greatly limits the types of geometries that can be practically realised.

Robotic fabrication has the potential to solve these construction challenges as the assembly of free-form geometry is simplified by virtue of a robot being able to place blocks in 3D space precisely. As such, the current goal is to advance the application of robotics in the context of fabricating free-form structural geometry – creating a fabrication-informed design process, which integrates structural efficiency and complex geometry with robotic fabrication.

This paper discusses the various components that are necessary for a fully informed design and fabrication process of a robotically assembled masonry vault: structural form-finding, brick pattern-definition, and robotic assembly. It presents the methodology of developing and implementing these topics simultaneously through exploration of both digital computation and physical prototyping, from initial small-scale tests to the construction of a large-scale doubly-curved glass brick vault (**Figure 1**). The vault is built using a cooperative robotic fabrication process, which allows the vault to be assembled without falsework or geometric templates - the geometry is defined such that the robots can provide all the temporary support. Since the vault was designed with fabrication and structural efficiency in mind, the geometry and brick tessellation are optimised to ensure a funicular form and account for the benefits and constraints of robotic fabrication (i.e. pick-up locations, placement sequence to avoid collisions and provide temporary support). This illustrates the importance of a non-hierarchical design process, in which the form is equally informed by structural and fabrication considerations.

2 State of the art

2.1 Self-supporting masonry

The robotic assembly method used for the vault in this project was inspired by various historical approaches to building masonry vaults without falsework. Timbrel vaults are a traditional construction style of Roman origin, which was introduced to the United States towards the end of the 19th century through the work of Rafael Guastavino (Ochsendorf 2010). This technique is based on using layers of brick or tile, bonded with mortar, to form a thin shell that works solely in compression (**fig. 2**). Notable characteristics of such vaults are that they can cover large distances and bear significant loads in relation to their thickness, and are executed without falsework, using guides where needed to inform the geometry of the vault. While timbrel vaults declined in use by the mid-20th century, their self-supporting characteristic has inspired recent investigations by various research groups (SOM and University of Alcalá 2019; Borne and et al. Heathcote 2016; Rippmann et al. 2012; Rippmann and Block 2013).

Another method for self-supporting vault construction is the historic barrel vault construction technique used by the Egyptians and Assyrians, and later the Byzantines (Choisy 1883), which relies on the frictional support provided by inclined courses to construct the vault without falsework. In this technique, successive courses are laid at an angle against a vertical end wall, with each course supporting the next (Heyman 1997).



Figure 2: Timbrel vault (Credits: SOM and University of Alcalá 2019).

2.2 Brick tessellation

Tessellating a surface is an exercise in mathematical mapping between two different domains, which in the architectural context can be thought of as producing a pattern on a surface while maintaining certain geometric properties (i.e. angles, distances, or areas). Geometric complexity aside, this process is further complicated when factoring in the physical constraints specific to masonry construction, such as keeping joint size and spacing within allowable tolerances while maintaining smooth courses of uniform bricks. While complex geometries were traditionally described empirically and built with guides, recent work has shown promising theoretical approaches for masonry tessellation, for example using a geodesic coordinate system to describe uniform bed joints on a free-form surface (Adiels 2016).

The task of tessellation for the proposed project is additionally constrained by the need for a geometry that is both self-supporting and can be constructed while considering robotic movement criteria. A recent method for generating translationally interlocked masonry geometries has been developed in the context of robotic construction (Loing et al. 2020). For our project, the tessellation scheme,

selected for its simplicity and uniformity, was based on the herringbone pattern, most famously used by Brunelleschi in the dome of the Florence Cathedral (Pizzigoni and Paris 2014; Paris et al. 2017; Pizzigoni et al. 2018). The support mechanism is achieved through the use of cross-layer bricks, which are required so that subsequent brick courses are supported by the layer below (as shown in Paris et al. 2020).

2.3 Structural form-finding and analysis

While there are numerous computational form-finding methods for structures – force density, dynamic relaxation, and particle-spring (Adriaenssens et al. 2014; Michiels and Adriaenssens 2018), to name a few – these have not been developed specifically for application in the design of masonry structures. The most well-known method suitable for free-form masonry structures is Thrust Network Analysis (TNA) (Block and Ochsendorf 2007; Block 2009), which is a 3D extension of graphic statics that ensures funicular (i.e. compression-only) solutions. The method was used in the construction of a free-form masonry vault at the Swiss Federal Institute of Technology (Davis et al. 2012).

The doubly-curved vault geometry used in this project is calculated from an approach based on graphic statics and the Airy's stress function. This technique was first proposed by Fraternali (2002), who in subsequent work implies a strong connection between his suggested polyhedral approximation of the Airy stress function and the TNA method (Fraternali 2010). There also exists an extension of this original discrete Airy stress function approach to a curvilinear coordinate system (Miki et al. 2015a,b). We use the discrete approach to find a function that satisfies all the criteria for a compression-only surface.

2.4 Cooperative robotic assembly

Robotic fabrication has the potential to address the construction challenges associated with complex geometries due to the robot's capacity of precisely positioning elements in 3D space. Masonry construction is one of the first construction methods that was adopted by the field of construction robotics, mainly due to the process predictability (identical elements placed in similar orientations). However, initial projects focused on the aesthetic qualities of controlled manipulation of the bricks' position and orientation (Bonwetsch et al. 2006, 2007) over generating structurally sound constructive elements. Further developments targeted self-supporting assemblies by including structural information but remained limited to vertical wall-elements and horizontal stacking of bricks (Piskorec et al. 2018). To expand the application of robotics in discrete element construction, we are targeting structural spanning geometries, such as vaults. In order to do so, we make use of

the robots' capacity for spatial assembly as proposed in various robotic fabrication projects (Volker et al. 2016; Parascho 2019). Furthermore, recent developments have explored the potential of using robots cooperatively to support each other during construction – a technique which shares some similarities with a chain-based method of providing temporary support to an unfinished vault (Deuss et al. 2014). For assembly purposes, cooperating robots allow for one robot to act as temporary support while the other robot is placing an element (Parascho et al. 2017; Thoma et al. 2018; Wu and Kilian 2018). We aim to apply this technique to masonry construction and expand robotic assembly methods towards structural applications.

2.5 Design for fabrication

Design for fabrication is an active area of research in the field of digital fabrication for structure-scale components. In additive manufacturing, for example, it is often a necessity that the geometry is informed by the fabrication process due to the inherent constraints associated with 3D printing. The constraints present in the construction of discrete masonry assemblies show similarities to those faced by continuous additive manufacturing, with several recent publications drawing parallels between the fields (Carneau et al. 2019; Motamedi et al. 2019; Carneau et al. 2020).

However, robotic assembly processes involve more complex constraints due to the six degrees of freedom design space of a robot. One strategy is to simplify the geometry of the structure to gain control over the unintuitive movement space of a robot. For example, many assembly projects use a layer-based rationalisation for the geometry which ensures that parts are reachable and no collisions occur (examples range from bricklaying projects (Bonwetsch et al. 2006) to wood assemblies (Oesterle 2009)). Not omitting geometric complexity (i.e. fully exploring the 6-dof design space) is crucial for unlocking the full potential of robots in fabrication. While studies were done to integrate path-planning techniques into the design process (Parascho et al. 2018), these rely on computationally expensive algorithms and large numbers of iterations. We address this challenge by working with the design space resulting from the fabrication constraints to generate the structure's geometry.

2.6 Summary

While robotic masonry construction has a long-standing tradition, this paper is based on the hypothesis that robotic masonry assembly can be implemented for structural applications beyond decorative uses. We thus aim to address the challenge of heavy-weight masonry construction for vault geometries by eliminating the need for support structures and searching for sequencing and form-finding methods that

ensure the structure's stability at all construction steps. The resulting research question revolves around finding a design method and workflow that can fully leverage the design space of robotic construction while fulfilling the hard constraints of compression-only geometries. Ultimately we aim to expand the design space for masonry construction beyond simplified non-structural geometries that are intuitively feasible.

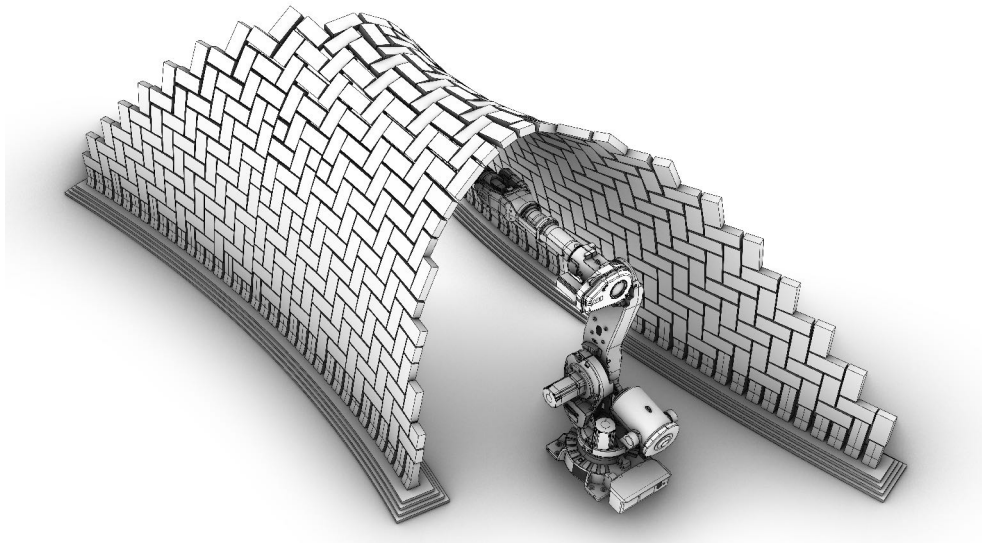


Figure 3: Finalized vault geometry.

3 Implementation

The project was developed on three levels simultaneously to avoid the inherent limitations of a hierarchical approach to design and fabrication. It thus consists of methods for: (1) structural design - including analysis and form-finding; (2) robotic fabrication - including material explorations, assembly choreography, sequence definition and path-planning; (3) geometric design - including pattern definition and overall form. The design of the vault is ultimately a result of the intersection of the geometric design-spaces of the structural form-finding and fabrication method. In the next sections, we illustrate the methods developed to identify these design spaces and convert them into geometric data. Finally, we show how the methods were implemented and tested through physical prototyping. The final vault geometry represents a doubly-curved, point-symmetric surface (fig. 3) which fulfills structural stability constraints and ensures collision-free robotic movements. The chosen material system consists of glass bricks bonded with a fast-setting Epoxy Putty (PIG™ Multi-Purpose Epoxy Putty) and standardised wedge elements.

3.1 Structural analysis

The preliminary shape of the vault was conceived as a series of leaning arches inspired by the barrel vault technique discussed in [sec. 2.1](#). But rather than having arches of similar base width, each arch base increases from the centre of the vault towards the ends to enhance lateral stability. The result is a doubly curved shell structure.

The precise analytical form of the vault was derived using the Airy's stress function form-finding approach as described in [sec. 2.3](#). In this process, form and force diagrams are established based on the principles of Graphic Statics (Baker et al. 2015; McRobie et al. 2015; Mitchell et al. 2015). The form diagram represents the plan projection of the vault structure that is calculated, and the force diagram reflects the forces in such a planar structure ([fig. 4](#)). If the vault is in equilibrium, then so is the structure obtained by projecting the forces onto a horizontal plane. The Airy's stress function is a three-dimensional function constructed in conjunction with the planar form diagram. The form and force diagram and the Airy's stress functions are all interrelated so that any change in one of the three affects the others. The Airy's stress function for the vault was constructed to ensure a smooth positive curvature at any point on the surface described by the function, which then results in a compression-only structure. The form and force diagrams are updated accordingly, and the third dimension (elevation) of the vault ([fig. 4](#)) is finally calculated using the force density method.

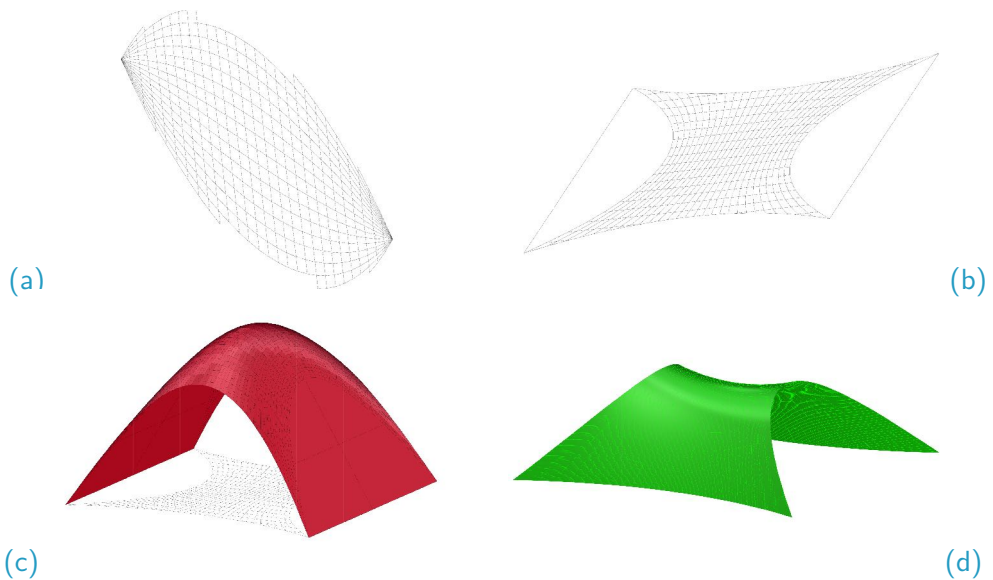


Figure 4: Form-finding process for the vault geometry (a) force diagram (b) form diagram (c) Airy's Stress function (d) vault shape.

We ensured that the specific shape and tessellation of the vault allowed for stable equilibrium states during all phases of construction. To accomplish this, we used both Limit State Analysis and Discrete Element Analysis approaches, which have been used successfully in previous work (Michiels et al. 2017). According to the Safe Theorem for masonry structures (Heyman 1966), equilibrium of a dome is guaranteed if a thrust line exists which lies entirely within the cross-section of the dome. In the limit state analysis the following assumptions, initially formulated by Heyman, were made: (1) no sliding of the bricks can occur; (2) the masonry has no tensile strength; (3) the masonry has infinite compressive strength. Besides the Limit State Analysis, we also performed numerical Discrete Element Analysis on each construction stage, using the commercially available software 3DEC (Itasca Consulting Group 2016). The Discrete Element Method models the performance of discontinuities and that of solid material, and can, therefore, simulate the collapse behaviour of the vault in all phases of construction. We modelled the glass brick/epoxy as a system of discrete rigid bodies (the bricks) with dry joint interfaces (the epoxy). Using these two methods in tandem, we established that the construction of the vault was safe throughout the entire construction process, without requiring any falsework.

3.2 Tessellation

The challenge of identifying a functional tessellation pattern combines geometry, structural stability and robotic fabrication constraints. The pattern directly influences tool design and path-planning strategies. We chose the herringbone pattern due to its interlocking brick system, which helped provide stability during construction. The bricks are placed orthogonal to one another and shifted by half their length at every row, as shown in [fig. 5](#).



Figure 5: Herringbone tessellation pattern with glass bricks in the constructed vault.

The distribution of the bricks in the herringbone pattern had to be refined to accommodate the amplified gap sizes at the scale of the final structure. The nature of the pattern makes it difficult to place discrete brick elements on a doubly-curved surface without leading to large gaps. The final vault geometry has a minimum radius of curvature of 1211 mm and 359 mm in the x- and y-planes, respectively (**fig. 6**). Without modification, the gaps of a uniformly distributed herringbone pattern on this geometry would have accumulated over the surface, eventually reaching a size of 49 mm, which cannot be economically filled with epoxy.

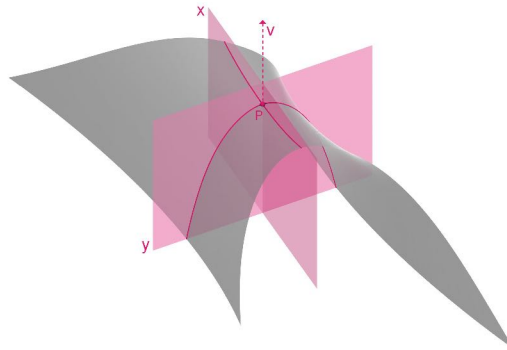


Figure 6: Vault surface with normal planes in directions of principal curvatures. Showing the x-plane, y-plane, point on vault surface, and vector at surface point P (Credits: Maciej Grzeskowiak (SOM), 2020).

To minimise the size of the gaps, we introduced two adjustments to the pattern definition by 1) adding *reset lines*, and 2) optimising the tessellation algorithm. The *reset lines* define vertical planes where the pattern is interrupted and started over - any horizontal brick that falls across this plane is replaced with two half-sized bricks to complete the vertical sections of the vault. The next row of bricks on the other side of the plane is added with a minimal vertical gap. The geometry of the support elements accommodates the resulting difference in length. We experimented with various locations of these reset lines and ultimately added four in the central part of the vault, which has the largest curvature value and hence the largest gap sizes (**fig. 7**).

To optimise the tessellation algorithm, instead of positioning each brick tangentially to the target surface at the brick's centroid point (**fig. 8a**), we used what we refer to as the *line and angle* method to define the position and orientation of the brick. The goal is to minimise vertical gaps in the structure (in y-direction) since these are significantly larger than horizontal ones. For this reason, the brick is moved such that the short edge surfaces intersect the vault normal sections in the y-direction (principal curvature direction) at their centroids (**fig. 8b**: points p and q.). Rotating around the axis p-q, an angle is found that aligns the brick with

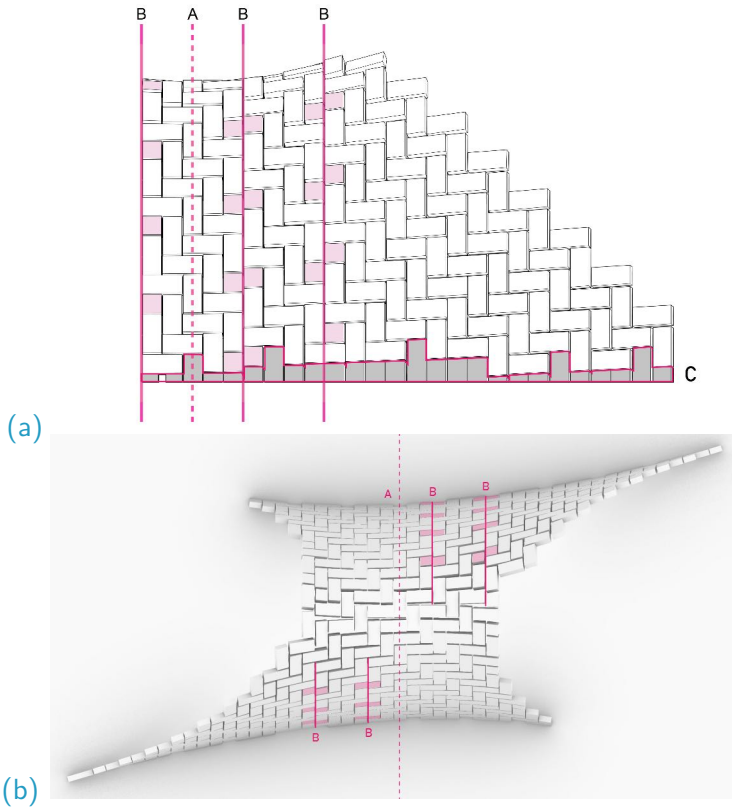


Figure 7: Reset lines that help shrink overall gap sizes in the: (a) prototype 6, and (b) final vault. Showing the middle arch (A) and reset lines (B), and the support elements (C).

the principal curvature tangent vector in x -direction (**fig. 8b**). We tested these strategies in three physical prototypes (discussed in the following section), which allowed us to identify further constraints for the geometry of the vault, namely a maximum curvature of $0.82 \times 10^{-3} \frac{1}{mm}$ in the x -plane and $2.78 \times 10^{-3} \frac{1}{mm}$ in the y -plane. This optimisation process ultimately resulted in 80% of the gaps between bricks in the final vault falling below 17.5 mm, which was set as the threshold for inserting an additional element into the gap to minimise epoxy use.

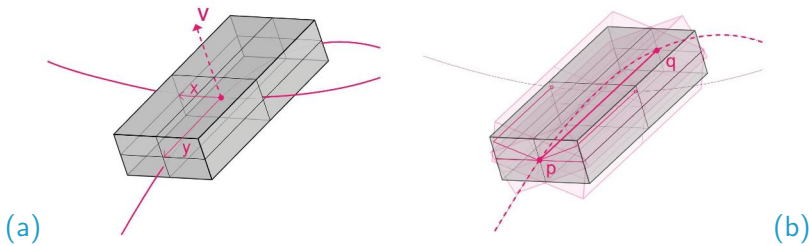


Figure 8: Brick alignment to vault surface. (a) centroid method (b) line and angle method.

3.3 Robotic fabrication

The cooperative robotic assembly technique lies at the core of the vault's development. To find a functioning assembly logic, we had to integrate the development of the robotic setup with constraints from the material system, brick pattern, sequencing, and overall vault geometry. As a result, the fabrication developments could not be restricted to robotic considerations alone but had to be developed in tandem with the other components of the project.

	Geometry	Tessellation	Brick	Robot	Connection
1	Arch	Running Bond	Wood	UR3	Modelling Compound
2	Arch	45° Herringbone	Composite	UR3	Epoxy Putty
3	Barrel Vault	90° Herringbone	Composite	UR3	Epoxy Putty 3D Printed Wedges
4	Doubly-Curved Vault	90° Herringbone	Wood	ABB 4600	Epoxy Putty Wood Wedges
5	Doubly-Curved Vault (Five Rows)	90° Herringbone	Recycled Glass Concrete	ABB 4600	Epoxy Putty Wood Wedges
6	Doubly-Curved Vault (Asymmetric)	90° Herringbone	Glass Concrete	ABB 4600	Epoxy Putty Wood Wedges
7	Arch	90° Herringbone	Glass	ABB 6640	Epoxy Putty
8	Doubly-Curved Vault (Symmetric)	90° Herringbone	Glass	ABB 6640	Epoxy Putty Acrylic Shim

Table 1: Prototypes built and construction parameters investigated.

We conducted a series of tests ([tab. 1](#) - a total of 8 prototypes) to investigate the relationship between structure, geometry and fabrication. Initial small-scale tests (1 - 3) focused on developing the overall assembly logic, robotic setup and the resulting physical design space for the structure. In the second series of prototypes (4 - 5), we aimed at scaling up the structure and fine-tuning the material system, sequence and robotic path-planning. The third and last series of prototypes (7 - 8) was conducted at the site of the exhibition and involved first testing a new robotic setup, followed by the construction of the final full-scale vault as a live demonstration. Only minimal geometric changes were made at this stage.

Small-scale prototyping

In a first step, we tested the alternating construction method on a simple arch consisting of a running bond brick assembly. Two small-scale UR3 robots, located

863.6 mm apart, were used to assemble the arch, which consisted of 13 bricks connected with air-dry modelling compound. The robots would alternate between placing a brick and supporting the existing arch (**fig. 9**).



Figure 9: Small-scale prototype to test the alternating placement strategy for a brick arch with a running bond pattern.

Besides serving as proof of concept for the assembly technique, this first test explored the geometric relationship between: 1) the location, 2) the orientation and dimensions of the arch, 3) the distance between the robots, 4) the robots' reach and collision-free movement range, and 5) the dimension and orientation of the tool. This information was ultimately used to define the volumetric design space of the vault geometry. The result is a saddle-shaped surface spanning over the two robots centred around a middle arch that lies in the common intersection volume of the two robots' reach spheres (**fig. 10**). The arch has a span of 827.9 mm and a height of 355.9 mm (in this small-scale configuration).

The subsequent small-scale prototypes explored expanding the arch into a surface-like geometry by testing different patterns and connection strategies. Taking references from traditional tiling patterns discussed in **sec. 2.2**, we first tested a 45° rotated herringbone pattern to laterally extend the arch geometry (**fig. 11a**) but switched to an orthogonally-oriented pattern (**fig. 11b**), which proved to be more stable during construction. While this tessellation had the benefit of generating local interlocking support between bricks with the capacity for spatial extensibility, it came with challenges in adjusting to a doubly-curved geometry, as discussed in **sec. 3.2**.

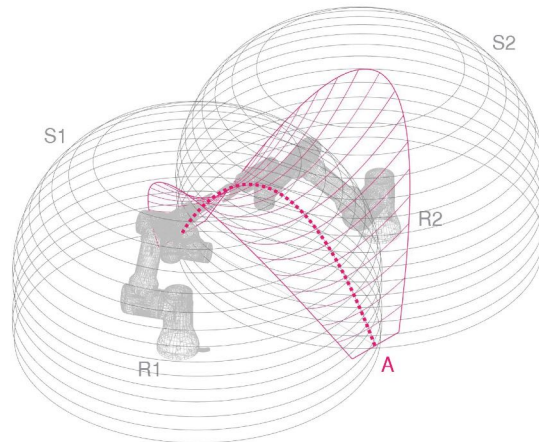


Figure 10: Small-scale prototype to determine the volumetric design space, showing the middle arch (A), the two robots (R1 & R2), and the two reachability spheres with grippers (S1 & S2).

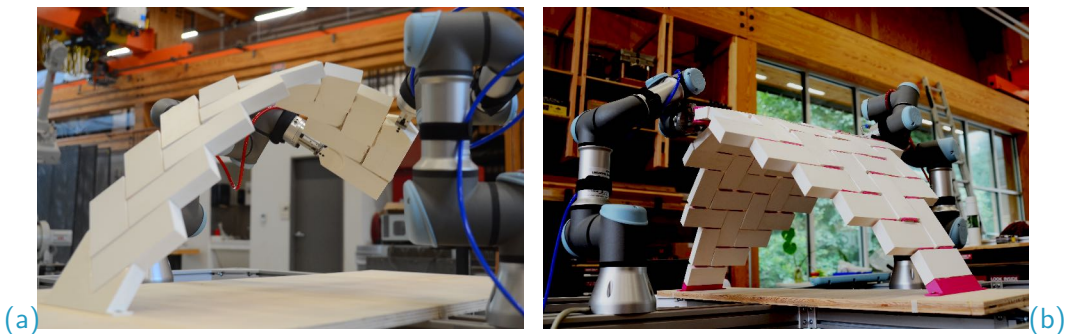


Figure 11: Herringbone tessellation options: (a) 45° (b) orthogonal.

Traditional masonry construction typically uses mortar as connection material, to strengthen the connection between the bricks and account for material and placement imprecision. However, we faced a different geometric challenge resulting from the double curvature of the vault geometry ([fig. 3](#)). To adjust to the different curvatures, the gaps between the bricks varied widely in terms of dimension and shape. Since the geometry of these gaps could be well predicted, we tested the use of 3D-printed wedges to minimise the volume of necessary adhesive material ([fig. 12b](#)). The wedges proved successful, but it became clear that they would be expensive to fabricate and complicated to place correctly in a full-scale structure.

Large-scale prototyping

The aim of the large-scale prototypes was to test the construction process at the full construction scale, using a larger robotic setup with two ABB 4600 robotic arms, mounted 3.5 m apart and with a reach of 2.55 m ([fig. 13](#)). This included experimenting with different brick materials and dimensions (wood, glass and

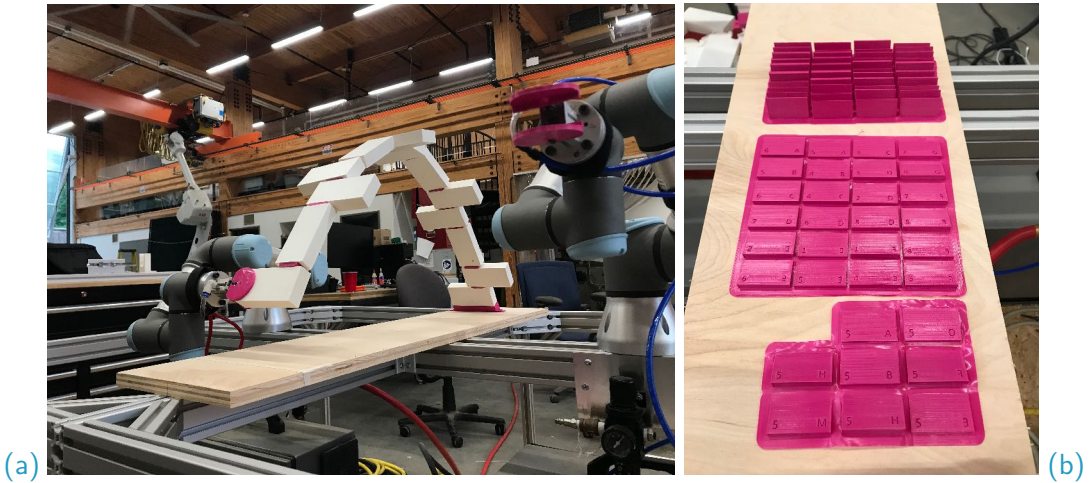


Figure 12: Middle arch construction with orthogonal tessellation: (a) Repeating 3-brick sequence, (b) 3D-printed wedges for gaps in arch.

concrete bricks of approx. 100 × 200 × 50 mm). Ultimately, together with digital simulations, the goal of this physical prototyping process was to identify the limitations of the full-scale fabrication method and feed this information into the design process to finalise the vault design. We conducted three separate tests to scale up the construction in controllable steps. Besides scale and material, the following methods were developed to ensure a successful building process: robotic path-planning for collision-free movements, patterning of the doubly-curved surface, and sequencing of the herringbone pattern to ensure reachability and stability throughout construction.

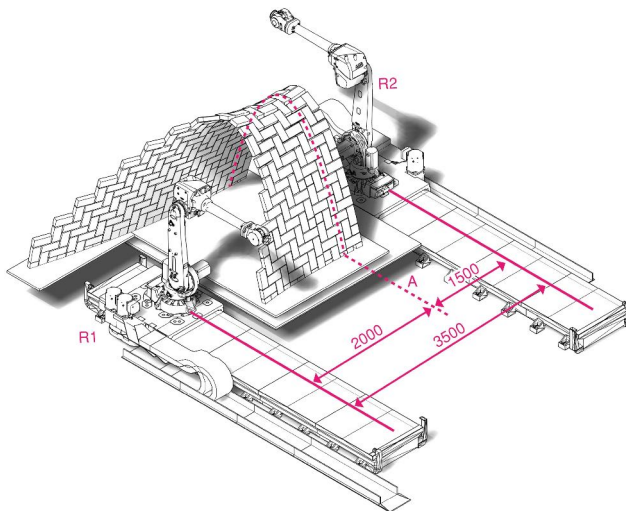


Figure 13: Robot location and brick pick up station in lab prototype 6, showing the middle arch (A) and the two robots (R1 & R2).

In the first prototype (**fig. 14**), we utilised wooden bricks to test solely the scalability of the robotic process. Shifting to glass bricks proved to be challenging due to the weight of the material and the low friction of the polished surface. In prototypes 5 and 6 (**fig. 15** and **16**) we focused on adapting the construction process to solve the challenges related to this material change, which are discussed in detail in companion publication. For these prototypes, we chose to work with a mix of glass and concrete bricks, since concrete has similar properties to glass (in terms of density and brittleness) and was more readily available. In all large-scale tests we used the same epoxy putty and opted for standardised wooden wedges, instead of the more costly custom 3D-printed ones, to fill out larger gaps. The wooden bricks measured 201 mm x 102 mm x 49 mm while the glass and concrete bricks used in these tests measured 246 mm x 116 mm x 53 mm.

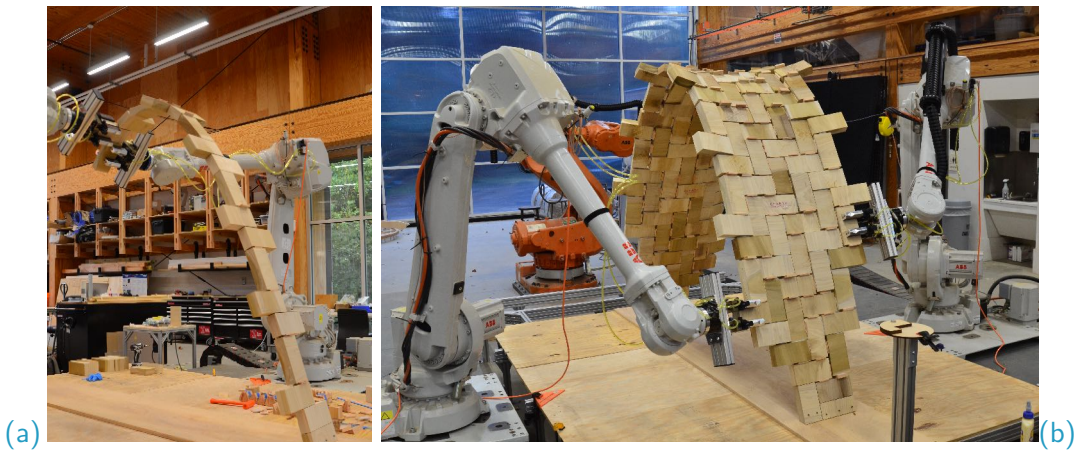


Figure 14: Large-scale wooden prototype of central section of the vault: (a) Middle arch construction. (b) Finished prototype.

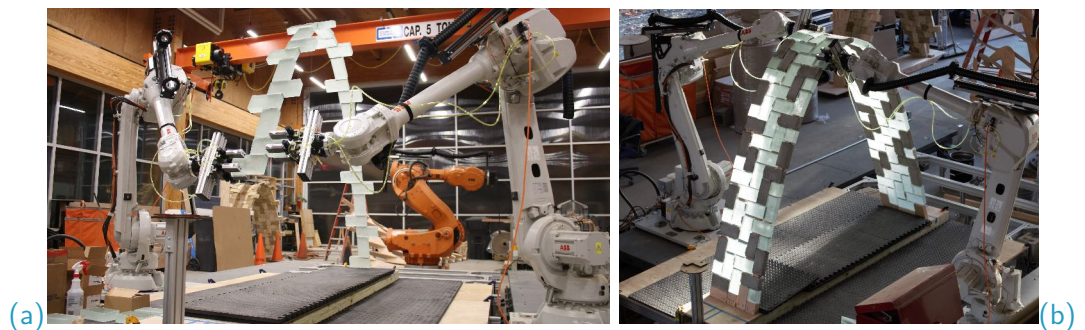


Figure 15: Large-scale glass/concrete prototype of central section of the vault: (a) Middle arch construction. (b) Finished prototype.

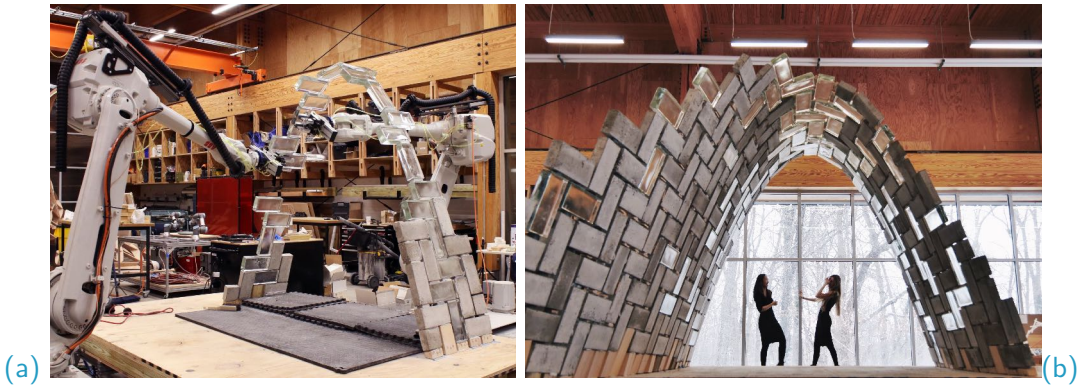


Figure 16: Large-scale glass and concrete brick prototype of partial vault: (a) Middle arch construction. (b) Finished prototype (Credits: Shenhan Zhu (CREATE Laboratory), 2019).

Similar to the small-scale prototypes, the size of the central arch in the large-scale prototypes is defined by the overlapping reach volumes between the two robots. During the experimentation with these prototypes, we found the ideal distance between the robots (each with a reach of 2.55 m) to be 4.0 m, which is what was ultimately implemented in the final construction setup. However, since we were constrained by the established 3.5 m placement in the Princeton University testing facility, we opted to shift the centre of the prototype by 0.5 m to one side to accurately reproduce the distance to the robot for one half of the structure (fig. 13). Based on this 4.0 m distance between the robotic arms, and the constraints of their reach, the maximum dimensions for the central arch resulted in 2.0 m height and 2.6 m span.

The construction sequence consists of two major parts: a strong central arch as a backbone (fig. 17a-c) and a point-symmetric vault extending towards both sides (fig. 17d-l). The central arch is structurally challenging to build since the two robots alternate in the role of temporary support and placing a new brick. To increase the lateral stability of the linear arch, first, a few extra bricks are placed at both ends of the arch to form a stable triangular base (fig. 17a-b). Once the central arch is finished, two extra rows of bricks are added on each side to form a strong five-row central spine (fig. 17c). The rest of the construction follows a *diagonal stepping* logic to help transfer weight down through the existing structure (fig. 17d-l).

The *diagonal stepping* construction sequence is different at either side of the same tessellation (fig. 18) due to the orientation of the Herringbone pattern. The guiding principle is to 1) have only two glueing sides - bottom and side - when a brick approaches the existing structure (from direction i in fig. 18) to easily apply

connections and 2) avoid alternating between horizontal and vertical bricks (fig. 18. H & V.) as much as possible for better control of robot configuration.

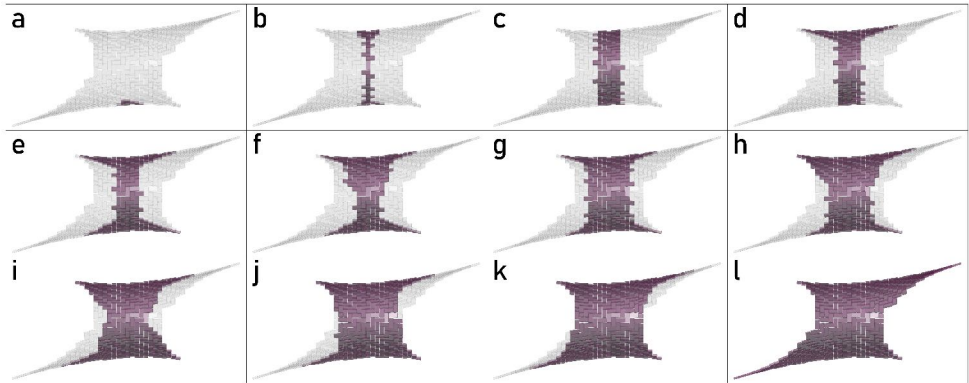


Figure 17: Construction sequence.

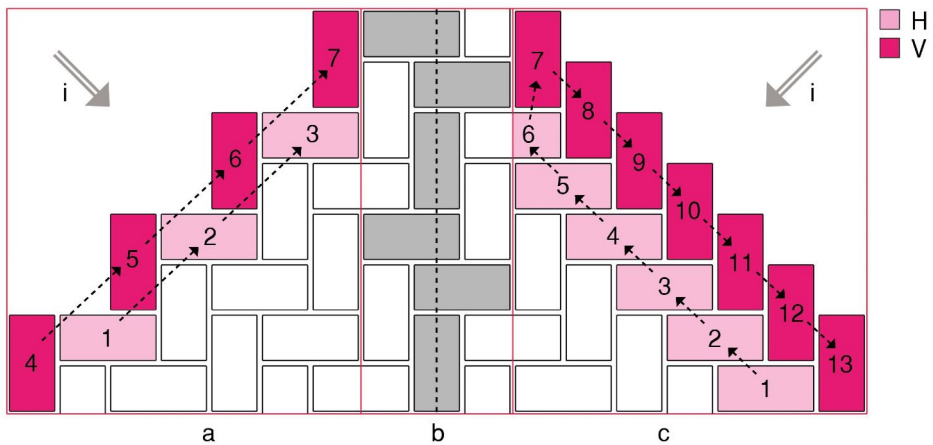


Figure 18: Diagonal stepping construction sequence, showing the two diagonal stepping patterns (a & c), the middle arch (b), the brick insertion direction (i), and the alternating layers of horizontally (H) and vertically (V) oriented bricks.

The path-planning of the robotic arm movements is defined by the following factors: the risk for collision between robot arm and existing structure, robot reachability in the required configuration, and the precise position and orientation of the individual bricks. Between picking up a new brick from one of the pick-up stations (fig. 19. B1 - B4.) and placing it in its final location and orientation, the robots go through movements that could lead to collisions with the existing structure. This is mainly due to the large number of configurations (a maximum of eight for six-axis robots with spherical wrists) that the robot can reach a given position and orientation in.

When simulating the robotic path for critical bricks (e.g. hard-to-reach bricks at the top, bottom, and edge of the vault) using ABB's RobotStudio software (ABB 2020), we found that the robot elbow (between axis four and axis three) is at high risk of colliding with the front of the existing structure when placing bricks on the back side and vice-versa. To increase the configuration predictability and lower risks of collision, we combined two measures: 1) we modified the vault geometry into an asymmetric shape and 2) we added a fixed "transition point" between every pick-up and placement pose. The asymmetry with regards to the longitudinal axis of the vault results in more freedom of movement for the robot elbow joint. The overall point-symmetry of the vault is a result of the two robots being rotated by 180 degrees and not physically mirrored. Overall, the path-planning combines the parametric placement of hundreds of bricks on the vault surface with the fixed "transition point" and pick up station locations lowering the risks for collision and adding predictability during the construction process.

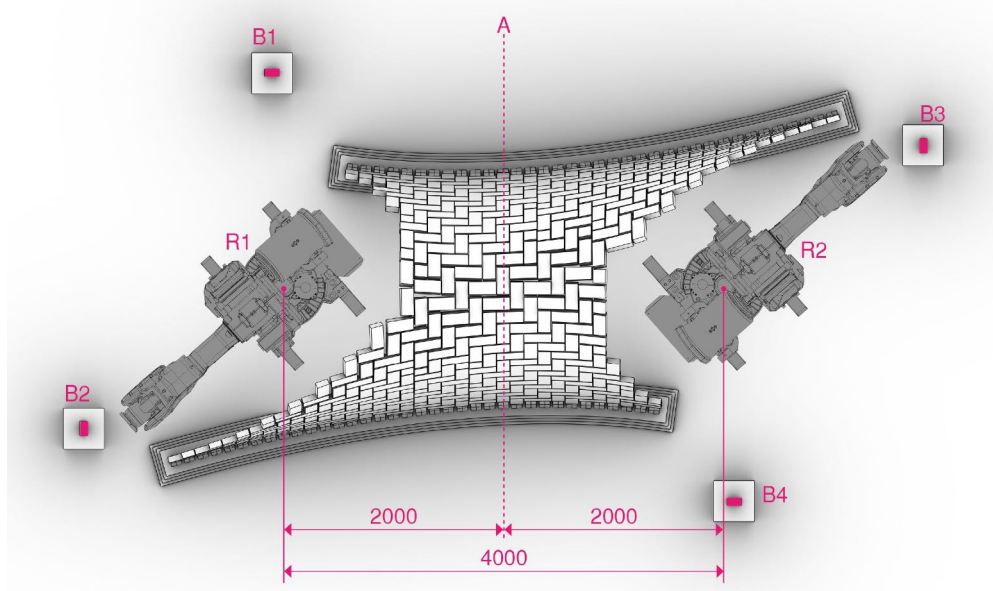


Figure 19: Robot location and brick pick up station for final vault construction setup, showing the middle arch (a), and the four brick pick up stations (B1 - B4).

4 Final vault construction

The physical implementation of the developed methods with respect to material, scale, robotic setup, path-planning, patterning and sequencing – were used to define a measurable geometric solution space for the construction of the full-scale glass vault. The final vault geometry (fig. 20 and 21) was constructed as a live

demonstration over the course of two weeks at the "Anatomy of Structure" exhibit hosted by Ambika 3 Gallery, Westminster University London. Given the on-site fabrication, all methods developed in the lab setting had to be easily adjustable to a new location. Thus, all identified design constraints were modelled as flexible parameters.

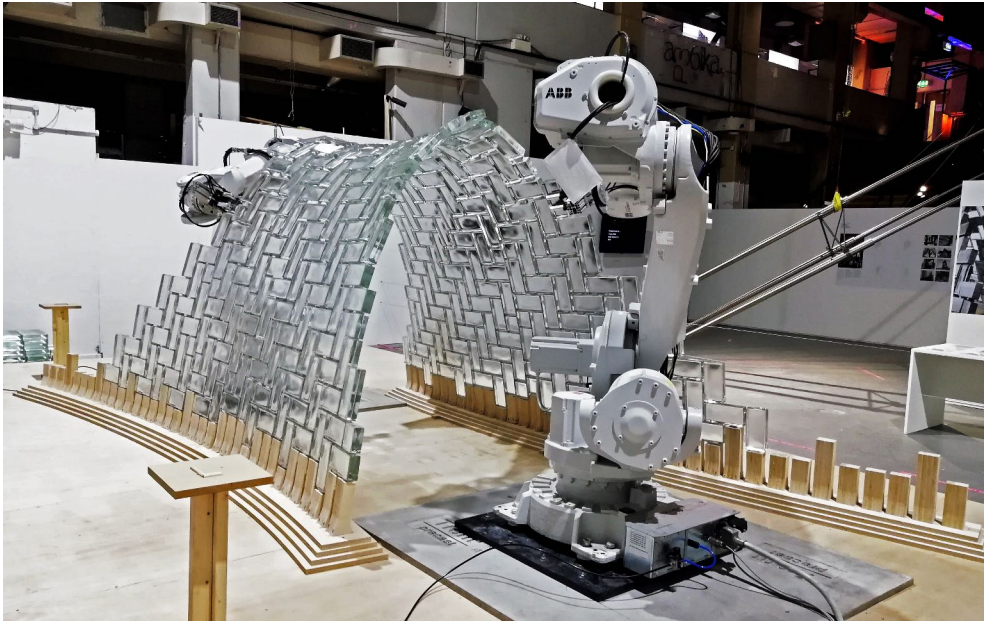


Figure 20: Final constructed vault: perspective view.

The setup in London included two ABB 6400 robotic arms, with an identical reach of 2.55 m as the robots used in the prototype construction in the Princeton University testing facility. The ideal distance for overlapping reach-volumes was identified as 4 m; thus the design space was extended to a volume of approximately $4.8 \times 7.8 \times 2.3$ m with an overlapping area of 2.6×1.6 and 2.0 m in height. As a result of the path-planning and reachability constraints, the middle arch had to be 1.9 m high, while the rest of the vault had to become taller, the closer it got to the robots' position to avoid collisions. The planned total number of bricks for the vault was 448 (419 full bricks and 29 half bricks). However, the construction of the vault was executed during the beginnings of the COVID-19 pandemic, which required us to stop the building process early. We thus adjusted the construction plan to finish a stable portion of the vault consisting of 338 glass bricks (309 full bricks and 29 half bricks; approx. $3/4$ of the planned full size), which weighed approx. 1400 kg.

The preliminary robotic calibration and tests were conducted at the Global Robots Facility, after which the two IRB 6640 robots were shipped and installed on pre-cast concrete pad footings place in the exhibition space. The nature of the tessellation was such that different heights of bricks were needed at this interface with the foundation. For simplicity, these were prefabricated from wood.

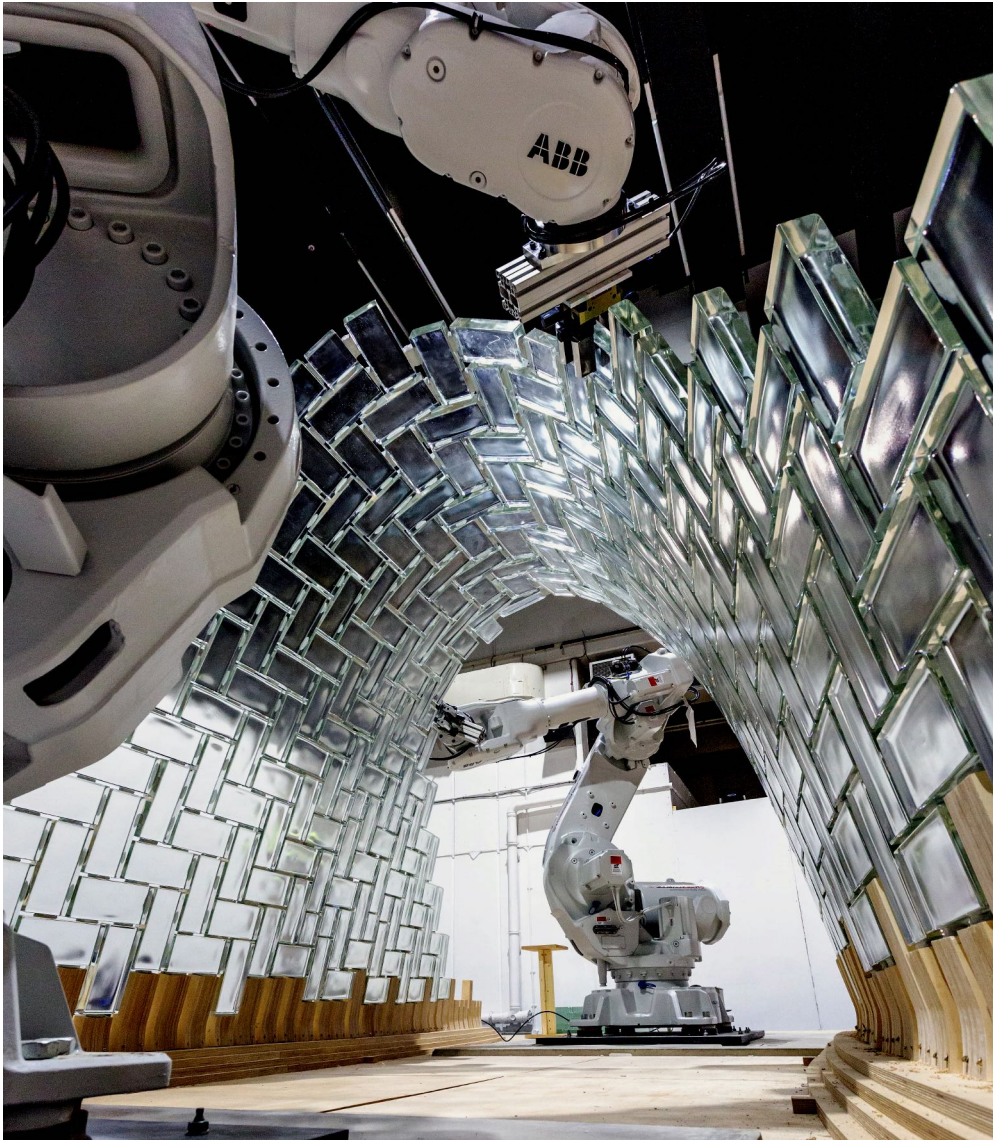


Figure 21: Final constructed vault: inside view (Credits: Maciej Grzeskowiak (SOM), 2020).

5 Conclusion

In this paper, we presented the successful development of a cooperative robotic assembly method for three-dimensional masonry structures. By combining structural form-finding and analysis methods with the implementation and testing of robotic assembly methods, we were able to expand robotic masonry construction to structural vault geometries. We showed that by analysing the individual design-spaces resulting from structural and fabrication requirements – defining their intersection prior to the design of the vault geometry – one can generate geometries that make use of the robots' full movement range while avoiding collisions.

Future work will address expanding the range of self-supporting geometries, for example by building assemblies without glued connections, relying solely on geometry and robots for stability. This could be achieved by adding more robots for support and fine-tuning the robotic construction sequence. In addition, we aim to achieve a closer integration of structural analysis into the design process, to inform both form and sequence directly. A streamlined design interface connecting structural analysis and fabrication simulation would enable adjusting the geometry to fulfil structural and fabrication constraints during its generation. Furthermore, by allowing the robots to dynamically adjust their roles in the construction process, we could achieve a much closer integration of the machine into the design, thereby maximising its potential.

Acknowledgements

This project would not have been possible without the support of academic and industry partners: the TU Delft Glass & Transparency Research Group, Poesia Glass Studio and Global Robots Ltd. Furthermore, the construction of the LightVault was only feasible through the many people that supported our research through administration, development and construction. We would like to acknowledge Lukas Fuhrmann, Chase Galis, Lisa Ramsburg and Ian Ting (CREATE Lab Princeton), Grey Wartinger and William Tansley (Princeton School of Architecture), Michael Cascio, Max Cooper, Dave Horos, Dmitri Jajich, Stuart Marsh, Mark Sarkisian, Matteo Tavano and Arthur Sauvin (Skidmore, Owings & Merrill).

We would also like to acknowledge the Metropolis Project of Princeton University, and the Princeton Catalysis Initiative for supporting this project.

References

- ABB (2020). RobotStudio. <https://new.abb.com/products/robotics/robotstudio>.
- Adiels, E. (2016). Structural influence of the geometry of masonry vaults - Brick tiling patterns for compression shells using geodesic coordinates. Master's thesis, Chalmers University of Technology.
- Adriaenssens, S., P. Block, D. Veenendaal, C. Williams, P. Block, D. Veenendaal, and C. Williams (2014, March). *Shell Structures for Architecture: Form Finding and Optimization*. Routledge.
- Baker, W., A. McRobie, T. Mitchell, and A. Mazurek (2015). Mechanisms and states of self-stress of planar trusses using graphic statics, Part I: Introduction and background. In *Proceedings of IASS Annual Symposium 2015*, Amsterdam, pp. 12.
- Block, P. (2009, May). *Thrust Network Analysis: Exploring Three-dimensional Equilibrium*. PhD Thesis, Massachusetts Institute of Technology, Cambridge, MA, USA.
- Block, P. and J. Ochsendorf (2007, December). Thrust Network Analysis: A new methodology for three-dimensional equilibrium. *Journal of the International Association for Shell and Spatial Structures* 48(3), 167–173.
- Bonwetsch, T., F. Gramazio, and M. Kohler (2007). Digitally Fabricating Non-Standardised Brick Walls. In *ManuBuild*, pp. 191–196.
- Bonwetsch, T., D. Kobel, F. Gramazio, and M. Kohler (2006). The informed wall: Applying additive digital fabrication techniques on architecture. *Synthetic Landscapes - ACADIA 2006 International Conference*, 489–495.
- Borne, E. and E. et al. Heathcote (2016, nov). The Droneport Project. L'Architecture d'Aujourd'hui Perspectives.
- Carneau, P., R. Mesnil, N. Roussel, and O. Baverel (2019, October). An exploration of 3d printing design space inspired by masonry. In *Proceedings of IASS Annual Symposium 2019*, Barcelona. Publisher: Zenodo.
- Carneau, P., R. Mesnil, N. Roussel, and O. Baverel (2020, August). Additive manufacturing of cantilever - From masonry to concrete 3D printing. *Automation in Construction* 116, 103184.
- Choisy, A. (1883). *L'Art de bâtir chez les Byzantins*. Paris: Société anonyme de publications périodiques. OCLC: 2070155.

- Davis, L., M. Rippmann, T. Pawlofsky, and P. Block (2012, nov). Innovative Funicular Tile Vaulting: A prototype in Switzerland. *The Structural Engineer* 90(11), 46–56.
- Deuss, M., D. Panozzo, E. Whiting, Y. Liu, P. Block, O. Sorkine-Hornung, and M. Pauly (2014, November). Assembling self-supporting structures. *ACM Transactions on Graphics (TOG)* 33(6), 214:1–214:10.
- Fraternali, F. (2010, March). A thrust network approach to the equilibrium problem of unreinforced masonry vaults via polyhedral stress functions. *Mechanics Research Communications* 37(2), 198–204.
- Frick, U., T. V. Mele, and P. Block (2015). Decomposing Three-Dimensional Shapes into Self-supporting, Discrete-Element Assemblies. In *Modelling Behaviour*, pp. 187–201. Cham: Springer International Publishing.
- Heyman, J. (1966, April). The Stone Skeleton. *International Journal of Solids and Structures* 2(2), 249–279.
- Heyman, J. (1997). *The Stone Skeleton: Structural Engineering of Masonry Architecture*. Cambridge University Press.
- Itasca Consulting Group, I. (2016). 3DEC — Three-Dimensional Distinct Element Code.
- Livesley, R. K. (1992, September). A computational model for the limit analysis of three-dimensional masonry structures. *Meccanica* 27(3), 161–172.
- Loing, V., O. Baverel, J.-F. Caron, and R. Mesnil (2020, May). Free-form structures from topologically interlocking masonries. *Automation in Construction* 113.
- McRobie, A., W. Baker, and T. Mitchell (2015). Mechanisms and states of self-stress of planar trusses using graphic statics, Part III: Applications and extensions. In *Proceedings of IASS Annual Symposia 2015*, Amsterdam, pp. 12.
- Michiels, T. and S. Adriaenssens (2018, January). Form-finding algorithm for masonry arches subjected to in-plane earthquake loading. *Computers & Structures* 195, 85–98.
- Michiels, T., R. Napolitano, S. Adriaenssens, and B. Glisic (2017, October). Comparison of thrust line analysis, limit state analysis and distinct element modeling to predict the collapse load and collapse mechanism of a rammed earth arch. *Engineering Structures* 148, 145–156.
- Miki, M., T. Igarashi, and P. Block (2015a, August). Direct application of Airy stress

- functions to NURBS patches for computing compression shells. In *Proceedings of the IASS Annual Symposium 2015*, Amsterdam, pp. 10.
- Miki, M., T. Igarashi, and P. Block (2015b, July). Parametric self-supporting surfaces via direct computation of airy stress functions. *ACM Transactions on Graphics* 34(4), 89:1–89:12.
- Mitchell, T., W. Baker, and A. Mcrobie (2015). Mechanisms and states of self-stress of planar trusses using graphic statics, part II: the Airy stress function and the fundamental theorem of linear algebra. In *Proceedings of IASS Annual Symposia 2015*, Amsterdam, pp. 12.
- Motamedi, M., R. Oval, P. Carneau, and O. Baverel (2019). Supportless 3D Printing of Shells: Adaptation of Ancient Vaulting Techniques to Digital Fabrication. In *Proceedings of the Design Modelling Symposium Berlin*, Berlin, pp. 714–726.
- Ochsendorf, J. A. (2010). *Guastavino vaulting: the art of structural tile*. New York: Princeton Architectural Press.
- Oesterle, S. (2009). Performance as a design driver in robotic timber construction. In T.-W. Chang, E. Champion, S.-F. Chien, and S.-C. Chiou (Eds.), *CAADRIA 2009. Proceedings of the 14th conference on computer-aided architectural design research in Asia*, pp. 665 – 672. National Yunlin University of Science and Technology Department of Digital Media Design. CAADRIA 2009; Conference Location: Taiwan, China; Conference.
- Parascho, S. (2019). *Cooperative Robotic Assembly: Computational Design and Robotic Fabrication of Spatial Metal Structures*. Ph. D. thesis, ETH Zurich.
- Parascho, S., A. Gandia, A. Mirjan, F. Gramazio, and M. Kohler (2017). Cooperative Fabrication of Spatial Metal Structures. In A. Menges, B. Sheil, R. Glynn, and M. Skavara (Eds.), *FABRICATE*, pp. 24–29. UCL Press.
- Parascho, S., T. Kohlhammer, S. Coros, F. Gramazio, and M. Kohler (2018). Computational design of robotically assembled spatial structures. a sequence based method for the generation and evaluation of structures fabricated with cooperating robots. In L. Hesselgren, A. Kilian, S. Malek, K.-G. Olsson, O. Sorkine-Hornung, and C. Williams (Eds.), *AAG 2018: Advances in Architectural Geometry 2018*, Wien, pp. 112 – 139. Klein Publishing.
- Paris, V., A. Pizzigoni, and S. Adriaenssens (2020, July). Statics of self-balancing masonry domes constructed with a cross-herringbone spiraling pattern. *Engineering Structures* 215, 110440.

- Paris, V., A. Pizzigoni, and G. Ruscica (2017, September). Brunelleschi's herringbone hidden reciprocal structure and the form finding of its self-supporting bricks. In *Proceedings of IASS Annual Symposia 2017*, Hamburg.
- Piskorec, L., D. Jenny, S. Parascho, H. Mayer, F. Gramazio, and M. Kohler (2018). *The Brick Labyrinth*, pp. 489–500. Springer.
- Pizzigoni, A. and V. Paris (2014). Herringbone, Gualandrino and Brunelleschi's Bricks. In *9th International Masonry Conference*, Guimarães.
- Pizzigoni, A., V. Paris, M. Pasta, M. Morandi, and A. Parsani (2018, July). Herringbone naked structure. In *Proceedings of IASS Annual Symposia 2018*, Boston.
- Rippmann, M. and P. Block (2013, September). Funicular Shell Design Exploration. In *Proceedings of the 33rd Annual Conference of the ACADIA*, Waterloo/Buffalo/Nottingham, Canada.
- Rippmann, M., L. Lachauer, and P. Block (2012, December). Interactive Vault Design. *International Journal of Space Structures* 27(4), 219–230.
- SOM and University of Alcalá (2019). Beyond the Limits (Exhibit).
- Thoma, A., A. Adel, M. Helmreich, T. Wehrle, F. Gramazio, and M. Kohler (2018). Robotic Fabrication of Bespoke Timber Frame Modules. In *Robotic Fabrication in Architecture Art and Design 2018*, Robotic Fabrication in Architecture, Art and Design 2018, pp. 447–458. Springer.
- Volker, H., M. Knauss, T. Kohlhammer, F. Gramazio, and M. Kohler (2016). Additive robotic fabrication of complex timber structures. In *Advancing Wood Architecture: A Computational Approach*, pp. 232. Routledge. Library Catalog: www.researchgate.net.
- Whiting, E. J. W. (2012). *Design Of Structurally-Sound Masonry Buildings Using 3D Static Analysis*. PhD, MIT, Boston.
- Wu, K. and A. Kilian (2018). Robotic equilibrium: Scaffold free arch assemblies. In *Recalibration on Imprecision and Infidelity - Proceedings of the 38th Annual Conference of the Association for Computer Aided Design in Architecture, ACADIA 2018*, pp. 342–349.